Water Research 292 (2026) 125288

Contents lists available at ScienceDirect

Water Research

journal homepage: www.elsevier.com/locate/watres

Biofiltration, seasonality, and distribution system factors influence nitrifier communities in a full-scale chloraminated drinking water system

Sarah Potgieter [a], Solize Oosthuizen-Vosloo [b], Kathryn Langenfeld [c], Katherine S. Dowdell [a,d], Matthew Vedrin [a,e], Rebecca Lahr [f], Ameet J. Pinto [g], Lutgarde Raskin [a,*]

[a] Department of Civil and Environmental Engineering, University of Michigan, Ann Arbor, MI, USA
[b] Institute for Cellular and Molecular Medicine, Department of Immunology, Faculty of Health Sciences, University of Pretoria, Pretoria, Gauteng, South Africa
[c] Ecology and Evolutionary Biology Department, University of Michigan, Ann Arbor, MI, USA
[d] Department of Civil and Environmental Engineering, University of Utah, Salt Lake City, UT, USA
[e] Department of Civil, Architectural, and Environmental Engineering, The University of Texas at Austin, Austin, TX, USA
[f] Water Treatment Services, City of Ann Arbor, Ann Arbor, MI, USA
[g] Department of Civil and Environmental Engineering, Georgia Institute of Technology, Atlanta, GA, USA

HIGHLIGHTS

- Seasonal and spatial factors shaped nitrifier dynamics and nitrite accumulation.
- *Nitrosomonas* cluster 6a, *Nitrospira,* and comammox co-occurred throughout the system.
- Nitrifier MAGs in the biofilter effluent persisted through the distribution system.
- Distribution system water age influenced the spatial patterns of *Nitrosomonas* MAGs.
- Comammox showed seasonal variation and persisted post-chloramination.

GRAPHICAL ABSTRACT

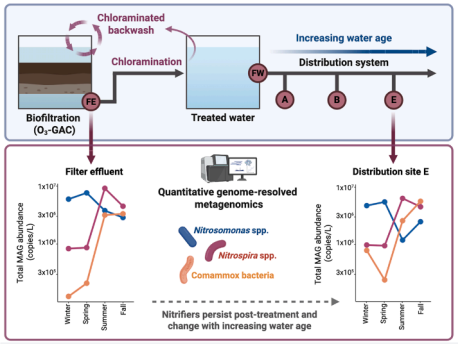

ARTICLE INFO

Keywords:
Biofiltration
Chloramination
Drinking water
Nitrification
Quantitative metagenomics
Droplet digital PCR

ABSTRACT

Nitrification in chloraminated drinking water systems has been widely studied, although limited information is available on the role of biofiltration in shaping the nitrifier communities within drinking water distribution systems (DWDS). Additionally, the co-occurrence of comammox and canonical nitrifiers in drinking water systems remains unclear. This study investigates how biofiltration shapes nitrifier communities in a full-scale drinking water system where chloramine is a secondary disinfectant, and biofilters are backwashed with chloraminated water. Samples were collected monthly for one year from biofilter effluent, finished water, and

Abbreviations: ANOVA, analysis of variance; AOA, ammonia-oxidizing archaea; AOB, ammonia-oxidizing bacteria; dbRDA, distance-based redundancy analysis; ddPCR, droplet digital PCR; DWDS, Drinking water distribution system; FE, Filter effluent; FW-Res, Finished water reservoir; GAC, granular activated carbon; NMDS, Non-metric Multidimensional Scaling; NOB, nitrite-oxidizing bacteria; MAG, metagenome assembled genome; PCoA, Principal coordinates analysis; PERMANOVA, permutational multivariate analysis of variance; RPKM, reads per kilobase million; WTP, Water treatment plant.

* Corresponding author.
E-mail address: raskin@umich.edu (L. Raskin).

https://doi.org/10.1016/j.watres.2025.125288
Received 15 September 2025; Received in revised form 24 December 2025; Accepted 27 December 2025
Available online 27 December 2025

three DWDS sites with varying water ages, water quality, and nitrite concentrations. Nitrifier abundances were quantified using droplet digital PCR, which showed contrasting temporal trends between the ammonia-oxidizing bacteria *amoA* gene and both nitrite-oxidizing bacteria 16S rRNA gene and comammox *amoB* gene abundances. Genome-resolved quantitative metagenomics revealed *Nitrosomonas* cluster 6a species, canonical *Nitrospira* species, and *Nitrospira*-like comammox species as the dominant nitrifiers. The same populations were detected in biofilter effluent and across DWDS sites, indicating that biofilter operation contributed to the persistence of nitrifiers in the DWDS. Further, DWDS site-specific factors, such as water age and disinfectant degradation, influenced the presence and abundance of individual nitrifier populations. These findings advance our understanding of how upstream treatment processes influence microbial community structure and nitrifier persistence in full-scale chloraminated DWDSs, and highlight the importance of considering biofilter operation, alongside disinfection practices, within integrated nitrification control strategies.

Introduction

Maintaining high microbial and chemical water quality standards within drinking water distribution systems (DWDSs) is essential for safeguarding public health. Chloramine, compared to chlorine, offers greater stability, providing prolonged protection against microbial growth and enhancing biofilm control in systems with high water age and dead-end mains (Lee et al., 2011). Chloramine also produces fewer regulated disinfection byproducts (Vikesland et al., 2001; Bougeard et al., 2010).

However, chloramine use has disadvantages, including the formation of nitrogenous disinfection byproducts (Bond et al., 2011) and the introduction of an additional source of ammonia, either through excess added ammonia during chloramine formation or through the release of ammonia via chloramine decay. This ammonia provides biologically available nitrogen that supports microbial growth and facilitates nitrification (Wahman and Pressman, 2014). In turn, microbial growth can accelerate chloramine decay and compromise the biological stability of DWDSs (Hossain et al., 2022).

Nitrification typically occurs in two stages, i.e., ammonia oxidation to nitrite by ammonia-oxidizing bacteria (AOB) and archaea (AOA), followed by nitrite oxidation to nitrate by nitrite-oxidizing bacteria (NOB). Alternatively, *Nitrospira*-like comammox bacteria can oxidize ammonia to nitrate (Pinto et al., 2016; Wang et al., 2017). Nitrite accumulation during nitrification is of particular concern, as elevated concentrations pose health risks (National Research Council 1995; Wilczak et al., 1996). As a result, regulatory limits have been established: the U.S. Environmental Protection Agency (EPA) set a maximum contaminant level for nitrite at 1 mg-N/L (US EPA 2024), the European Union directive 2020/2184 implemented a stricter limit of 0.5 mg-N/L (European Union (EU) 2020), and the World Health Organization established a health-based guideline of 3 mg/L as NO_2^- (World Health Organization 2017).

The dynamics of nitrifiers within full-scale DWDSs are complex. Multiple studies link changes in the identity and abundance of canonical nitrifiers to treatment processes (e.g., biofiltration and chloramination) and DWDS factors such as water age, pipe materials, and biofilm formation (Hossain et al., 2022; Zhang et al., 2009; Shi et al., 2020). Biofiltration, a widely applied drinking water treatment method, relies on biofilms on granular media to remove particulates, biodegrade natural organic matter, control taste and odor compounds, and reduce and remove certain contaminants (Basu et al., 2016; Bai et al., 2022). While biofiltration enhances water quality, it also inevitably introduces microbial cells into the DWDS, a natural consequence of the process that may be viewed as unfavorable from a water quality perspective (Pinto et al., 2012; LaPara et al., 2015; Ma et al., 2020). Therefore, it is important to understand which microorganisms are released downstream and how they shape DWDS communities. Operating conditions, including ozone pretreatment, backwashing, and disinfectant use, influence biofilter communities and performance (Laurent et al., 2003). However, the extent to which biofiltration specifically influences nitrifier communities in DWDSs remains unclear.

In addition to canonical nitrifiers, comammox bacteria have been discovered in drinking water biofilters (Pinto et al., 2016; Tatari et al., 2017; Vilardi et al., 2022) and DWDSs (Hossain et al., 2022). However, our understanding of their role in nitrification within full-scale drinking water systems is still limited. Questions remain regarding their niche differentiation, co-occurrence, and interactions with canonical nitrifiers, as well as responses to water quality drivers across seasonal timescales.

Therefore, this study investigated the persistence and complex dynamics of AOB, NOB, and comammox bacteria in a full-scale chloraminated drinking water system, considering the contribution of upstream biofiltration. As many utilities consider adopting GAC filtration to meet emerging regulatory requirements, understanding how upstream processes influence downstream nitrifier populations is critically important. This study moves beyond previous 16S rRNA gene-based surveys by providing quantitative, genome-resolved evidence of nitrifier occurrence throughout treatment and distribution. By integrating quantitative metagenomics with high-resolution droplet digital PCR (ddPCR), this study determined the absolute abundances of specific nitrifier taxa and tracked their population-level responses to treatment and seasonal variations. Together, these approaches provide a mechanistic understanding of nitrifier ecology in full-scale chloraminated systems, supporting the development of targeted monitoring and nitrification control strategies.

2. Materials and methods

2.1. Site description

This full-scale study was performed at the City of Ann Arbor drinking water treatment plant (WTP) and DWDS, Ann Arbor, MI, USA, as described by Pinto et al. (2012), Kotlarz et al. (2018), and Dowdell et al. (2024). In summary, the WTP serves approximately 125,000 residents and delivers an average of 13 million gallons per day (MGD). Source water comprises a mixture of surface water (80–85 %) and groundwater (15–20 %). Treatment includes two-stage lime softening, coagulation, flocculation, sedimentation, and ozone disinfection with a concentration × contact time (CT) of approximately 2 mg·min/L. Effluent from the ozone contactor flows to biofilters containing granular activated carbon (GAC) and sand. Monochloramine (approximately 3 mg-Cl_2/L) is added as the secondary disinfectant before the treated water enters the DWDS.

2.2. Sample collection and processing, and basic water quality monitoring

Samples from the filter effluent (FE), finished chloraminated water in the reservoir (FW-Res), and three sites within the DWDS (Sites A, B, and E) were collected monthly from November 2019 to November 2020, except for April 2020 due to the COVID-19 pandemic ($n = 49$). These samples correspond to those described by Dowdell et al. (2024). Sites A, B, and E were selected for this study based on their differences in water age and nitrification potential (Sites C and D, included by Dowdell et al. (2024), were not incorporated in the current study). Further site details are provided in Table S1. Briefly, FE samples were collected from the combined effluents of six filters following five minutes of flushing of the sampling port. FW-Res samples were collected from continuously

flowing sample taps in the WTP.

DWDS samples (Sites A, B, and E) consisted of cold water collected from sinks in three buildings after approximately 15 to 20 minutes of flushing and stabilization of temperature, oxidation-reduction potentail, and pH to ensure that the samples were representative of the DWDS water (Table S1). The three DWDS sample sites were part of the WTP compliance monitoring sites and were selected based on varying water ages, distance from the WTP, and history of nitrification. Water ages at the DWDS sites were estimated using the City of Ann Arbor's hydraulic model, which includes the use of an EPANET DWDS model (Dowdell et al., 2024; Rossman et al., 2020). All samples were collected in sterile 10 L Nalgene polycarbonate bottles and transported to the laboratory on ice.

Upon arrival in the laboratory, 8 to 10 L of bulk water sample was filtered through a STERIVEX™ GP 0.22 μm filter unit (MilliporeSigma, Burlington, MA, USA) to harvest microbial biomass. For each sampling event, 250 mL of UltraPure™ DNase/RNase-Free Distilled Water (Invitrogen) was filtered and processed as a negative control. Filter units were stored at −80 °C until DNA extraction was performed using a modified DNeasy PowerWater Kit® (QIAGEN) protocol. Modifications included lysozyme and proteinase K treatment, the addition of chloroform:isoamyl alcohol (24:1), and amended bead beating steps (Vosloo et al., 2019). DNA extracts were quantified using a Qubit™ dsDNA High Sensitivity (HS) Assay Kit (Thermo Fisher Scientific) and the Qubit™ 4 Fluorometer (Thermo Fisher Scientific) (Table S1 reports the DNA yield [ng/μl] for all samples). Each DNA extraction batch included a reagent-only extraction control. All DNA extracts (100 μl) were aliquoted and stored at −80 °C.

An additional 500 mL samples were collected at each sampling location for water quality monitoring (Table S2). Nitrate concentrations for surface and groundwater sources were also measured for this study. In addition, the WTP regularly quantified nitrite in the WTP and DWDS samples from 2014 to 2024. Note that free ammonia concentrations refer to the sum of ammonia (NH_3) and ammonium (NH_4^+) concentrations, but are simply referred to as ammonia in the rest of this manuscript.

2.3. Quantifying nitrifier populations with ddPCR

ddPCR analysis followed the guidance of the Minimum Information for Publication of Quantitative Digital PCR Experiments (Huggett, 2020). Targets included betaproteobacterial AOB (16S rRNA gene), *Nitrosomonas* cluster 6a (ammonia monooxygenase subunit A [*amoA*] gene), *Nitrospira* spp. (16S rRNA gene), and *Nitrospira*-like comammox clade A (ammonia monooxygenase subunit B [*amoB*] gene). Primers and probes (IDT, Integrated DNA Technologies, Inc., Coralville, USA) are shown in Table S3, indicating the use of either TaqMan probe-based or EvaGreen-based assays. Target nitrifier groups were based on previous knowledge of nitrifier diversity in the Ann Arbor drinking water system (Pinto et al., 2016; Vilardi et al., 2022), and the identification of dominant nitrifiers in the metagenomic dataset. Assays were performed with the QX200™ AutoDG Droplet Digital™ PCR System (Bio-Rad Laboratories, Inc., Hercules, CA). Reaction mixtures and cycle conditions for each assay are described in the supplemental text (Text S1). Reference gene sequences for each assay were synthesized as gBlocks® (IDT, Integrated DNA Technologies, Inc., Coralville, USA) for use as positive controls (Table S3).

Gene copies were adjusted for average copy number per cell, i.e., one gene copy for AOB and *Nitrospira* 16S rRNA genes, one gene copy for the comammox *amoB* gene (Vilardi et al., 2022; Hermansson and Lindgren, 2001; Dionisi et al., 2002), and three gene copies for the *Nitrosomonas* cluster 6a *amoA* gene (Yuichi et al., 2011; Bollmann et al., 2013; Kozlowski et al., 2016; Orschler et al., 2020). The *Nitrospira* 16S rRNA gene amplifies both comammox-*Nitrospira* and *Nitrospira*-NOB (Hermansson and Lindgren, 2001). Therefore, *Nitrospira*-NOB abundance was estimated by subtracting comammox bacteria *amoB* gene copies from *Nitrospira* 16S rRNA gene copies. Similarly, unassigned AOB (non-*Nitrosomonas* cluster 6a AOBs) abundance was estimated by subtracting *Nitrosomonas* cluster 6a *amoA* gene copies from AOB 16S rRNA gene copies.

2.4. Metagenomic sequencing, pre-processing, de novo co-assembly, and reconstruction of metagenome assembled genomes (MAGs)

Four samples from each location were selected for metagenomic sequencing, representing winter (December 2019), spring (March 2020), summer (July 2020), and fall (October 2020) ($n = 20$). Paired-end sequence libraries were prepared using NEBNext® Ultra™ II FS DNA Library Prep Kit for Illumina, and sequencing was performed using a SP lane on the NovaSeq 6000 system with 500 cycles at the Advanced Genomics Core, University of Michigan, Ann Arbor, USA. Negative controls (i.e., unused Sterivex filters, Sterivex filters treated with sterile, ultra-pure water, and extraction reagent blanks) were pooled and sequenced using Illumina MiSeq nano, 500 cycles. Sequencing data processing followed the workflow including, sequence processing, *de novo* co-assembly, and MAG reconstruction established by Vosloo et al. (2021) (Fig. S1) and are described in Text S2, Fig. S2, Table S4 and S5.

2.5. Quantitative internal standard spike-in and metagenomic quantification of nitrifier MAGs

Before library prep, synthetic dsDNA spike-ins (Sequins) (Hardwick et al., 2018) were added at 1.9 % of total DNA mass (Table S6). The absolute abundances of nitrifier MAGs were determined using QuantMeta with read depth variability and threshold read depth regressions generated specifically for this dataset (Langenfeld et al., 2025). Individual MAG absolute abundances were calculated as the mean absolute abundance of each contig normalized by length, with zeroes for contigs below detection. Results were converted to copies per liter (copies/L) using the DNA extraction elution volume (100 μL) and the filtered sample volume (Table S1).

2.6. Statistical analyses

Analyses were performed in R (version 4.2.1) (R Core Team 2021) and RStudio (Version 2023.09.1) (RStudio Team 2020). The normality of drinking water quality parameters and MAG abundances was evaluated using Q–Q plots (*car* package) and confirmed with the Shapiro–Wilk test (*stats* package). Correlation analysis was performed with the Kendall rank correlation method (τ), using the 'cor' function from the base *stats* package in R. Non-metric Multidimensional Scaling (NMDS) was performed using metaMDS provided in the *vegan* package (Oksanen et al., 2019) with Bray−Curtis dissimilarity distances. Permutational multivariate analysis of variance (PERMANOVA) was performed using the 'adonis' function in the vegan package. The drinking water quality parameters associated with community shifts were identified by distance-based redundancy analysis (dbRDA) based on Bray−Curtis dissimilarities, in the vegan package, addressing collinearity as described by Vosloo et al. (2021). Analysis of variance (ANOVA) was then used to test the significance of each response variable, and only response variables with significance were kept in the model. The explanatory value of significant response variables was determined with variation partitioning analysis using the varpart function in the *vegan* package. All plots were generated using *ggplot2* (Wickham et al., 2016).

3. Results

3.1. Spatial-temporal changes in ammonia, nitrite, and nitrate concentrations between the WTP and select DWDS sites

Sampling occurred monthly from December 2019 through November 2020 (excluding April, due to the COVID-19 pandemic). The highest

nitrite concentrations occurred in the FE sample in March 2020 (0.08 mg-N/L), when water temperatures were lowest across sample locations (mean ± standard deviation: 6.8 ± 1.7℃) (Fig. 1A and Table S1). At this time, elevated nitrite concentrations were also observed in the FW-Res and DWDS sites, likely due to carryover from the FE. Nitrite concentrations subsequently decreased for all samples through August 2020, as water temperatures increased (average of 21.7 ± 1.17℃ across sample locations), and remained low for the rest of the year for all samples, except for Site E (Fig. 1A and Table S1). The nitrite concentrations for Site E increased to 0.04 mg-N/L in October 2020, indicating incomplete nitrification. Site E also exhibited higher ammonia concentrations and lower monochloramine concentrations compared to other sites (Fig. 1A), suggesting chloramine decay linked to a higher water age.

Historical monitoring (2014–2024) showed similar trends (Fig. 1B). Contrasting trends in nitrite concentrations were observed between Site E and FW-Res, Site A, and Site B, with Site E having a higher estimated average water age (67.9 h) compared to Sites A and B (15.7 and 27.1 h, respectively). Nitrite concentrations in the FW-Res, Site A, and Site B increased in March and April (early spring) each year, coinciding with average water temperatures rising above 10℃ (11.3 ± 2.2℃). This trend was particularly pronounced in March 2021, when nitrite concentrations in the FW-Res peaked at 0.08 mg-N/L. Conversely, nitrite concentrations in the FW-Res decreased to near the limit of detection (0.005 mg-N/L) in August to November (late summer and fall), as water temperatures declined from summer peaks (~25℃) to an average of 18.2 ± 5.1℃. The same temporal trends were observed for Site A and Site B, with shorter water ages. However, the opposite was observed for Site E, where nitrite concentrations increased in September to November (fall) each year, exceeding 0.1 mg-N/L most years. The WTP proactively manages nitrite concentrations above 0.1 mg-N/L with increased monitoring and targeted flushing at affected sites.

In this study, nitrate concentrations in the source water and microbial nitrification influenced nitrate concentrations in the WTP and DWDS. Throughout the study year, nitrate concentrations at all sampling sites generally followed source water trends, indicating a continuous influence of source water on system-wide nitrate concentrations (Fig. S3). This was particularly apparent in December 2019 to March 2020, when nitrate concentrations in the FE, FW-Res, and DWDS sites closely mirrored those in the source water. The contribution of microbial nitrification became more pronounced from June to November 2020, when average nitrate concentrations across the FE, FW-Res, and DWDS sites (0.37 ± 0.12 mg-N/L) exceeded the average source water concentrations (0.19 ± 0.04 mg-N/L) for the same period. This indicated increased nitrate production in the WTP and DWDS. Additionally, a sharp increase in nitrate concentrations in late June coincided with a marked decline in nitrite levels, further supporting the conclusion that complete nitrification occurred during this period.

3.2. *Nitrosomonas and Nitrospiraspp. are the dominant nitrifier populations*

Sequencing of DNA extracts from 20 samples generated ~883 million 250-nucleotide paired-end reads (44,148,360.5 ± 7,300,757.5 reads per sample) (Table S4). Metagenomic data processing resulted in the construction of 668 MAGs (Text S2). Evaluation of the binning process showed that 87.53 ± 4.14 % of processed sequence reads were

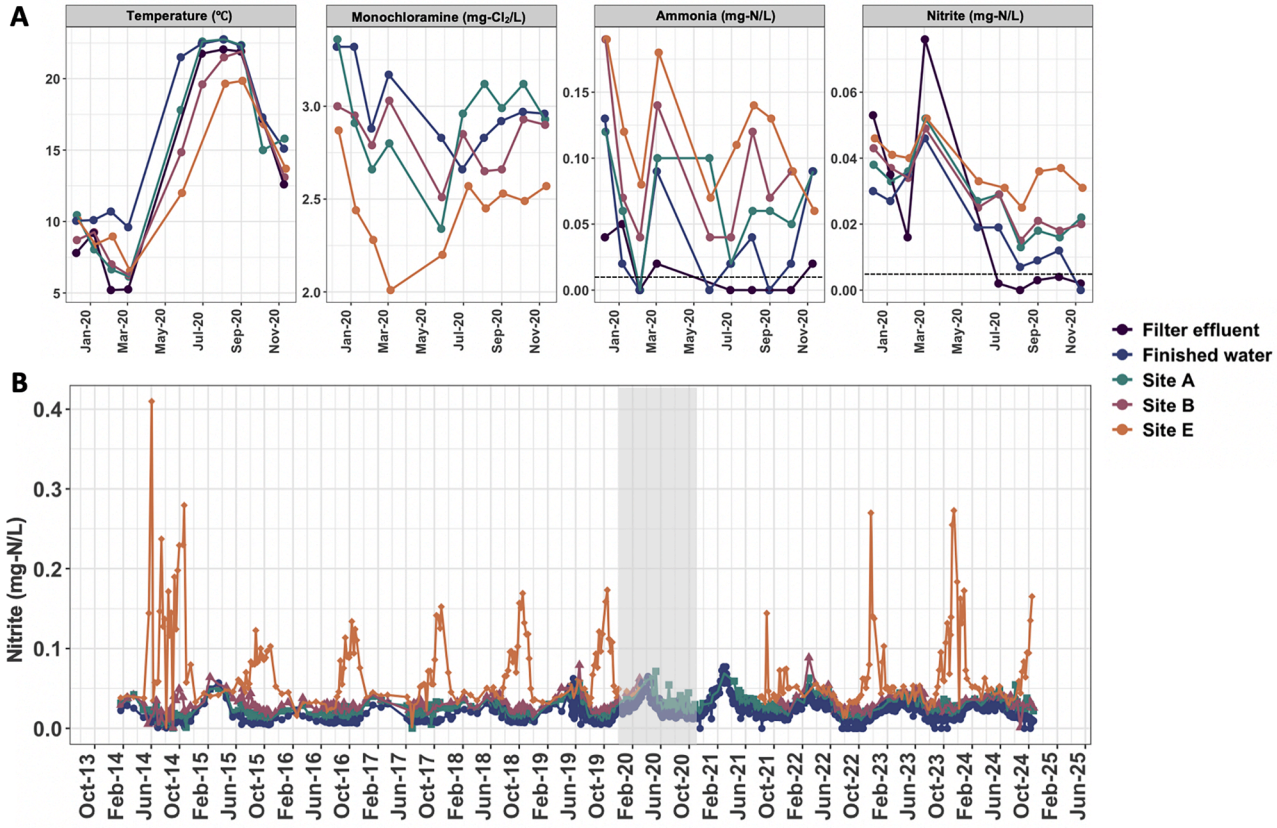

Fig. 1. (A) Temperature (℃), monochloramine (mg-Cl_2/L), ammonia (mg-N/L), and nitrite (mg-N/L) concentrations for the study period (December 2019 to November 2020) for filter effluent (FE), finished water reservoir (FW-Res), and DWDS sites (Sites A, B, and E). Limits of detection for the following water quality measurements: monochloramine (0.04 mg/L as Cl_2), ammonia (0.01 mg-N/L), and nitrite (0.005 mg-N/L), indicated by dashed lines (B) Historical nitrite concentrations (mg-N/L) from 2014 to 2024 for FW-Res and Sites A, B, and E. Monitoring of DWDS Sites B and E were suspended from April 2020 to August 2021 due to the COVID-19 pandemic. The grey area on the plot corresponds to the study period (Dec 2019 to Nov 2020). FE is not historically measured. The legend applies to both plots A and B. Source: Adapted from Potgieter et al. (2025).

retained in the 668 MAGs (Table S4). All 668 MAGs were classified as bacteria, and phylogenomic analysis revealed a diverse assemblage of taxa (Table S7), spanning 18 phyla, with *Pseudomonadota* (*Proteobacteria*), *Bdellovibrionota*, and "*Candidatus* Patescibacteriota" (*Patescibacteria*) constituting 47 %, 18 %, and 15 % of the total MAGs, respectively (Table S8).

Nine nitrifier MAGs were recovered, i.e., five *Nitrosomonas* and four *Nitrospira* spp. The quality and characteristics (i.e., completeness, redundancy, etc.) of these MAGs, as described by the minimal information metagenome-assembled genome requirements (MIMAG), (Bowers et al., 2017) are detailed in Table S9, together with the presence/absence of nitrification genes for each MAG. All *Nitrosomonas* spp. MAGs grouped within *Nitrosomonas* cluster 6a (Fig. 2A), (Orschler et al., 2020) and all *Nitrospira* spp. MAGs fell within *Nitrospira* sublineage II (Fig. 2B). Two *Nitrospira* MAGs grouped closely with *Nitrospira lenta* (*Nitrospira*-NOB), and the other two grouped closely with known clade A *Nitrospira*-like comammox. Notably, comammox MAG_117 grouped closely with a MAG that was previously assembled from the Ann Arbor WTP biofilters and was classified as belonging to the comammox clade A1 (*Nitrospira* sp. Ga0074138) (Pinto et al., 2016) (Fig. 2B). Comammox MAG_589 grouped closely with *Nitrospira* sp. ST-bin4, identified by Wang et al. (2017), and belongs to the comammox clade A2. Genome annotation confirmed that both comammox MAGs contained key ammonia oxidation genes (ammonia monooxygenase and hydroxylamine oxidoreductase) (Table S9).

3.3. Seasonal variations influence nitrifier abundances and microbial community structure

Metagenomic data revealed that all *Nitrosomonas* MAGs belonged to *Nitrosomonas* cluster 6a. Consequently, this group was specifically targeted using the *Nitrosomonas* cluster 6a *amoA* gene primer set with ddPCR (Text S3, Fig. S4 to S6) (Orschler et al., 2020; Harms et al., 2003). *Nitrosomonas* cluster 6a abundances were elevated in December 2019 through March 2020 (winter and early spring) with an average and standard deviation of $2.41\times10^7 \pm 1.16\times10^6$ gc/L across all samples, and were 10-fold lower in June to September 2020 (summer and early fall) ($2.18\times10^6 \pm 4.49\times10^4$ gc/L) when water temperatures exceeded 15 °C (Fig. 3 and Table S10). Their abundances had increased again in October 2020 ($4.02\times10^5 \pm 2.26\times10^5$ gc/L) before decreasing 10-fold in November 2020 ($9.11\times10^4 \pm 2.24\times10^5$ gc/L). The large standard deviations primarily reflect spatial variation across sampling locations rather than measurement uncertainty. Their abundances were negatively correlated with temperature ($\tau = -0.43$, $p < 0.001$), suggesting this group may be more competitive at lower temperatures, and positively correlated with nitrite concentrations ($\tau = 0.44$, $p < 0.001$). For example, their abundance spike in March 2020 corresponded to nitrite concentration spikes across sample sites, which was especially pronounced in the FE sample (Fig. 1). Additionally, their abundances exhibited limited correlations with ammonia concentrations but showed significant negative correlations with unassigned AOB abundances ($\tau = -0.35$, $p < 0.001$) (Table S11).

Temporal trends in unassigned AOB (non-*Nitrosomonas* cluster 6a AOBs) abundances were less pronounced. However, unassigned AOB were most abundant across all sample locations in July ($9.91\times10^6 \pm 4.85\times10^6$ gc/L) (Table S10), positively correlating with temperature ($\tau = 0.35$, $p < 0.01$) (Table S11). Unassigned AOB abundances frequently exceeded *Nitrosomonas* cluster 6a abundances, often displaying contrasting trends, most notable from June to October (Fig. 3).

Nitrospira-NOB and comammox were most abundant from June to September, showing negative correlations with *Nitrosomonas* cluster 6a *amoA* gene abundances ($\tau = -0.42$, $p < 0.05$ and $\tau = -0.16$, $p < 0.05$, respectively) (Fig. S7). However, *Nitrospira*-NOB abundances declined in October, coinciding with higher *Nitrosomonas* cluster 6a abundances. *Nitrospira*-NOB and comammox abundances were positively correlated ($\tau = 0.53$, $p < 0.01$; Fig. S7) and each showed a 10 to 100-fold higher average abundance from August to September compared to December to March (Fig. 3 and Table S10). Higher temperatures (>15 °C) favored the

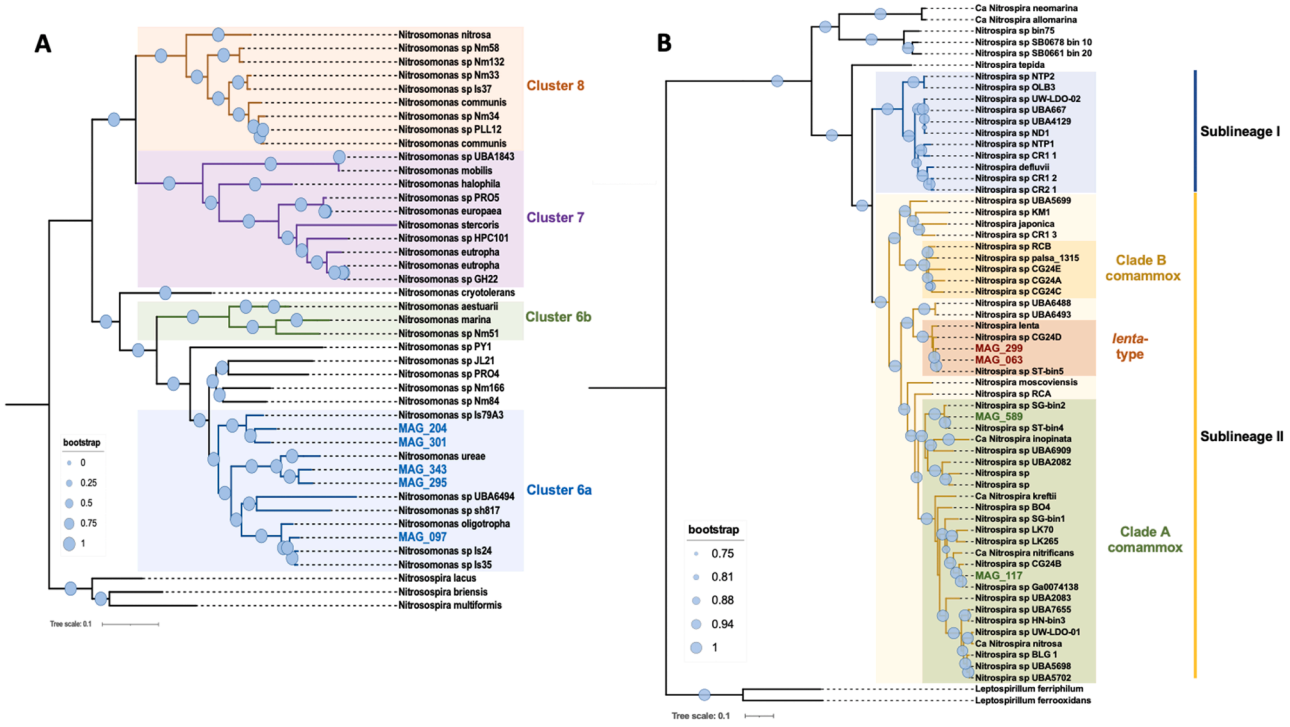

Fig. 2. Phylogenomic trees for nitrifier MAGs (bold, colored) obtained in this study with corresponding reference genomes (black). (A) Phylogenomic tree for *Nitrosomonas* MAGs (blue) and *Nitrosomonas* spp. reference genomes, with three *Nitrosospira* spp. genomes used as the outgroup. (B) Phylogenomic tree for *Nitrospira* MAGs (colored based on groupings) and *Nitrospira* spp. reference genomes, with two *Leptospirillum* spp. reference genomes used as the outgroup. Bootstrap values are indicated as circles at each node of the trees, with the legend included at the bottom left of each tree. Source: Adapted from Potgieter et al. (2025).

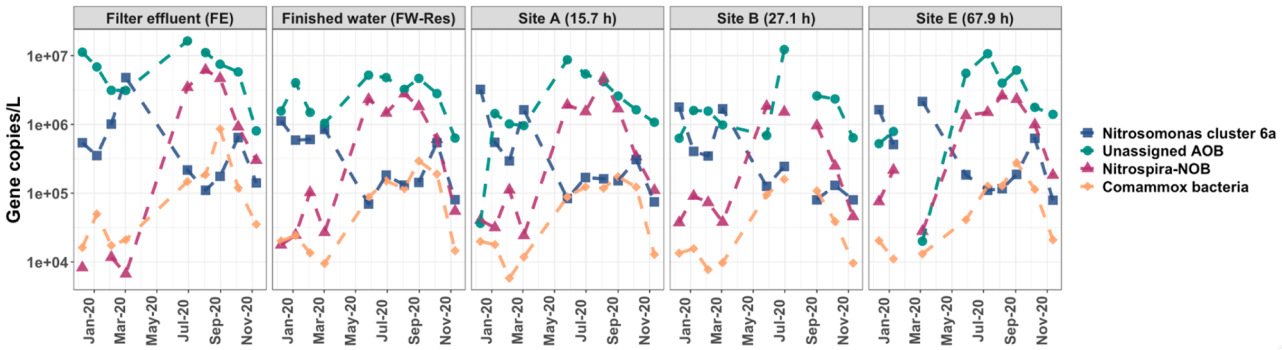

Fig. 3. ddPCR results (gene copies/L) for *Nitrosomonas* cluster 6a *amoA* gene (blue), non-*Nitrosomonas* cluster 6a betaproteobacterial AOB 16S rRNA gene (unassigned AOB: green), *Nitrospira* 16S rRNA gene (*Nitrospira*-NOB: red), and comammox bacteria *amoB* gene (orange) across the sample locations for one year. Approximate water age (in hours) is indicated in the top banner for DWDS Sites A, B, and E. Missing data (Aug: Site B and Feb: Site E) result from insufficient DNA extracted for ddPCR amplification. Additionally, sampling was not possible in April for all locations due to the COVID-19 pandemic. Source: Adapted from Potgieter et al. (2025).

growth of both *Nitrospira* groups, with *Nitrospira*-NOB and comammox gene abundances correlating positively with temperature ($\tau = 0.67$, $p < 0.001$ and $\tau = 0.59$, $p < 0.001$, respectively) (Table S11). Additionally, from June to September, comammox gene abundances were similar to or even exceeded those of *Nitrosomonas* cluster 6a *amoA* genes.

Our data show that the addition of chloramine between the FE and the FW-Res did not substantially reduce ddPCR nitrifier gene copy abundances (Fig. 3 and Table S10). Trends for most gene targets at the FW-Res and Sites A, B, and E followed those of the FE samples. Gene abundances in the FE were significantly correlated with downstream sites for several nitrifying groups (Fig. S7). Notably, *Nitrospira*-NOB in the FE showed strong and significant correlations across most sites, with the highest at Site A ($\tau = 0.89$, $p < 0.001$). The *Nitrosomonas* cluster 6a *amoA* gene abundances also exhibited strong correlations, particularly between FE and FW-Res ($\tau = 0.72$, $p = 0.006$) and between FE and Site E ($\tau = 0.71$, $p = 0.014$). Similarly, comammox *amoB* gene abundances in the FE correlated well across all sites, with significant associations at each location. In contrast, unassigned AOB abundances in the FE showed significant correlations only with FW-Res ($\tau = 0.67$, $p = 0.013$) (Fig. S7). While DNA-based analyses cannot distinguish between viable and non-viable cells, the differing group- and site-specific correlations (rather than uniform downstream persistence of all populations) indicate ongoing nitrifier activity rather than passive DNA transport of extracellular DNA. Site-specific changes in nitrite concentrations further support this assertion. Overall, the data indicate consistent downstream persistence of key nitrifiers, particularly comammox and *Nitrospira*-NOB, from the FE into the DWDS.

NMDS, based on Bray-Curtis dissimilarity, revealed strong temporal trends within the 668 MAGs (Fig. S8A), with PERMANOVA confirming that seasonality (PERMANOVA: $R^2 = 0.427$, $p < 0.003$) explained more of the variation than spatial differences (PERMANOVA: $R^2 = 0.109$, $p < 0.688$). Bray–Curtis dbRDA linked seasonal clustering of the microbial community with key water quality parameters (Permutation test for Bray–Curtis dbRDA, all $p = 0.001$) (Fig. S8B). Communities were structured along environmental gradients defined by total chlorine, temperature, pH, and nitrate. Total chlorine (monochloramine) was positively associated with winter samples. In contrast, temperature aligned with summer samples and negatively correlated with nitrite, total dissolved solids (TDS), and conductivity, variables that were collinear and thus followed similar trends. Spring communities aligned with higher nitrate concentrations, while pH positively correlated with ammonia. These findings indicate that seasonal community dynamics are driven by interacting water quality factors, often acting in tandem through collinearity.

3.4. Pre-disinfection treatment shapes nitrifier communities, with species abundances shifting across DWDS sites

Nitrifier MAG absolute abundances (as copies/L) strongly correlated with MAG reads per kilobase million (RPKM) abundances ($\tau = 0.76$, $p < 0.001$) (Fig. S9). All nitrifier MAGs were detected in the FE samples, indicating that the pre-disinfection dynamics, including biofiltration, influenced DWDS nitrifiers. Among the *Nitrosomonas* MAGs, MAG_295, MAG_301, and MAG_204 were the most abundant, with consistent trends across all sampling locations (Fig. 4 and Table S12). Like *amoA* gene abundances obtained by ddPCR, these three *Nitrosomonas* MAGs were highest in December and peaked in March across all samples. In contrast, their abundances were lower in July and October. Seasonal shifts in dominance were apparent among *Nitrosomonas* MAGs, with MAG_295 being most abundant in March, while MAG_301 became more predominant in July and October. Interestingly, *Nitrosomonas* MAG_343, though less abundant than the dominant *Nitrosomonas* MAGs, exhibited a notable decline in July with increasing water age. Particularly at Site E, MAG_343 decreased approximately 1000-fold. MAG_097 showed notable spatial dynamics, increasing in abundance with water age, and rising 100-fold from the FE samples to abundances comparable to other dominant MAGs at Site E. MAG_097 also exhibited trends distinct from other *Nitrosomonas* MAGs, particularly at Sites A and B, where it was less abundant in March and more abundant in July. Except for MAG_097, all *Nitrosomonas* MAGs displayed negative correlations with temperature ($\tau = -0.39$ to -0.57, $p < 0.001$) and positive correlations with nitrite concentrations ($\tau = 0.31$ to 0.55, $p < 0.01$) (Fig. S10). *Nitrosomonas* MAG_097 showed limited correlations with water quality parameters.

Nitrospira-NOB MAGs (MAG_299 and MAG_063) exhibited consistent spatial and temporal trends from the FE through DWDS sites (Fig. 4 and Table S12). Their abundances in the DWDS mirrored those in the biofilters, with minimal impact from chloramination or DWDS-specific factors such as water age. In contrast to most *Nitrosomonas* MAGs, both *Nitrospira*-NOB MAGs remained low in December and March. Their levels peaked in July and decreased slightly in October. This trend was consistent with *Nitrospira* 16S rRNA gene abundance data obtained through ddPCR (Fig. 3). The similar trends for these two MAGs likely stem from their close grouping with *N. lenta* (Fig. 2B), suggesting that they may belong to the same species with similar metabolic capabilities. Both MAGs correlated positively with temperature ($\tau = 0.70$, $p < 0.001$) and negatively with ammonia ($\tau = -0.42$, $p < 0.05$) and nitrite concentrations ($\tau = -0.5$, $p < 0.01$) (Fig. S10).

Between the two comammox MAGs (MAG_117 and MAG_589), MAG_117 typically dominated and, like the *Nitrospira*-NOB MAGs, showed consistent spatial trends from the FE through the DWDS sites (Fig. 4 and Table S12). Both comammox MAGs showed seasonal patterns

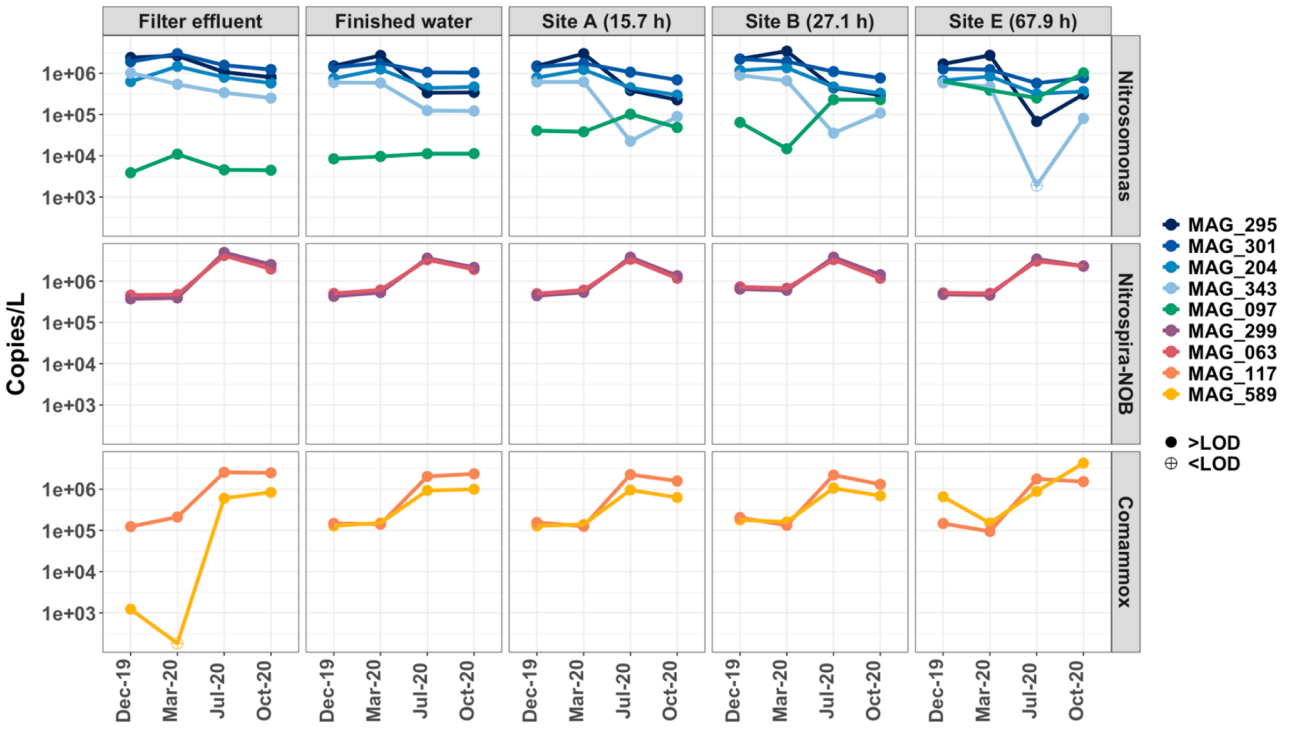

Fig. 4. The absolute abundances as copies per liter (copies/L), determined using QuantMeta, for MAGs identified as *Nitrosomonas* spp. (MAG_295, MAG_301, MAG_204, MAG_343, and MAG_097), *Nitrospira*-NOB (MAG_299 and MAG_063) and comammox bacteria (MAG_117 and MAG_589) across all sample locations. Approximate water age (in hours) is indicated in the top banner for DWDS sites. Specific MAGs are noted in the legend on the right. Open circles indicate MAG absolute abundances in which <10 % of contigs within a MAG were above detection. Source: Adapted from Potgieter et al. (2025).

with higher abundances in July and October compared to December and March, following the same trends observed with *Nitrospira*-NOB MAGs. MAG_589 exhibited notable spatial variation across the system, with particularly low abundance in the FE samples in December and March compared to MAG_117. In contrast, MAG_117 remained consistently abundant in the FE throughout the year, consistent with its close phylogenetic grouping with a comammox species previously identified in the same system (Pinto et al., 2016) (Fig. 2B), suggesting its persistence in the biofilters. MAG_589 abundance increased following chloramination, reaching concentrations similar to MAG_117 in the FW-Res and at Sites A and B in December and March, indicating a response to post-disinfection conditions. At Site E, MAG_589 exceeded both MAG_117 and *Nitrospira*-NOB abundances in December and became the most dominant nitrifier in October. Both comammox MAGs correlated positively with temperature ($\tau = 0.59$ to 0.72, $p < 0.05$). MAG_117 showed negative correlations with ammonia ($\tau = -0.5$, $p < 0.01$) and nitrite concentrations ($\tau = -0.6$, $p < 0.001$), while MAG_589 showed no significant correlations with these parameters (Fig. S10).

4. Discussion

4.1. Temporal trends in nitrifier dynamics

The seasonal variations in nitrifying bacteria abundances (ddPCR and quantitative metagenomics) help explain the temporal fluctuations in nitrite concentrations within the DWDS. Nitrifier growth rates and substrate utilization efficiencies vary by species and environmental conditions, including temperature, pH, and ammonia concentrations (Nowka et al., 2015; Sakoula et al., 2021). Although *Nitrosomonas* spp. grow optimally from 20 °C to 30 °C (Garrity et al., 2005; Yang et al., 2022), they have been found across a broader temperature range, from 4 °C to 40 °C, in drinking water (Itoh et al., 2013; Ma et al., 2023). In this study, *Nitrosomonas* spp. were most abundant in late winter and early spring, when water temperatures ranged from 5 °C to 10 °C. This was evident in March, when high abundances of AOB, particularly *Nitrosomonas* cluster 6a, were observed alongside peak nitrite concentrations in the FE, while *Nitrospira*-NOB and comammox bacteria were comparatively low.

While AOB abundances remained consistently high throughout the winter months (December 2019–March 2020), *Nitrospira*-NOB were much less abundant, leading to incomplete nitrification and nitrite accumulation due to their slower growth rates and lower energy yields from nitrite oxidation at low temperatures (Nowka et al., 2015; Daims et al., 2016). AOB persistence during colder periods may be supported by their establishment within biofilter microbial communities (LaPara et al., 2015; Laurent et al., 2003; Ma et al., 2023; Andersson et al., 2001), enabling a rapid restart of nitrification in the spring as water temperatures begin to rise (Andersson et al., 2001). Additionally, less frequent backwashing of the biofilters during colder periods, due to lower biological activity, and continuous seeding from the influent water may further support their persistence in the biofilters. Additional factors such as higher ammonia availability, reduced competition, and increased dissolved oxygen levels may also favor AOB during the winter (Hossain et al., 2022; Pintar and Slawson, 2003).

In contrast, both *Nitrospira*-NOB and comammox increased in late summer and early fall, consistent with their reported growth ranges of 10 °C to 47 °C (Yang et al., 2022; Sakoula et al., 2018), and that temperature has a positive effect on *Nitrospira* spp. (Fowler et al., 2018). During this period, nitrite concentrations had decreased from their March peak, suggesting that excess nitrite was oxidized to nitrate or that nitrite production was limited due to the complete oxidation of ammonia to nitrate by comammox bacteria. While higher NOB abundance typically implies effective nitrite oxidation, the absence of viability or activity measurements limits confirmation that these populations were actively oxidizing nitrite. Furthermore, elevated nitrite levels, most notable at Site E, in late summer and early fall, coincided with higher *Nitrospira*-NOB abundances. This observation could be attributed to the affiliation of the two *Nitrospira* MAGs with the species

N. lenta, which is known for its lower affinity for nitrite and limited tolerance to high nitrite concentrations (Sakoula et al., 2018). Additionally, Site E experienced increased ammonia concentrations, likely due to monochloramine decay, thereby providing more ammonia for oxidation to nitrite by AOBs. These observations highlight how seasonal and site-specific factors, together with species-specific physiological traits, drive nitrification dynamics in drinking water systems.

4.2. Persistence of nitrifiers from biofilters into the DWDS

Although ozone is applied as a primary disinfectant in this system, it also oxidizes natural organic matter into more biodegradable compounds, increasing the availability of assimilable organic carbon entering the GAC filters (Goel et al., 1995). Additionally, no ozone residual is carried over to the biofilters; therefore, no disinfectant is applied directly to the GAC filter medium. As a result, the filters function as biologically active carbon filters capable of sustaining robust biofilm communities. Previous work at this utility has also shown that the ozonated water entering the filters contains a low but measurable fraction of viable microorganisms, further supporting biofilm development (Kotlarz et al., 2018; Dowdell et al., 2024).

Beyond the clear temporal trends, this study also revealed that the biofilters influenced nitrifier dynamics throughout the DWDS. Previous studies have shown that biofilters influence the bacterial community composition in downstream drinking water by seeding biomass into the FE (Pinto et al., 2012; LaPara et al., 2015; Ma et al., 2020). In this study, nitrifier MAGs were consistently detected in the FE, FW-Res, and throughout the DWDS, showing persistence through treatment and distribution. Notably, the tracking of nitrifier MAGs from biofilters to finished water and into the DWDS provides a novel genomic perspective on their persistence and potential for seeding downstream DWDSs. Nitrifiers in the FE are likely "leaky colonizers" (Pinto et al., 2012), which are present in biofilms on GAC media where they form a stable reservoir of biomass that periodically sloughs into the effluent and seeds the DWDS (LaPara et al., 2015; Daims et al., 2015; Rosenqvist et al., 2023). These findings underscore the need to consider biofiltration practices when developing nitrification control strategies in chloraminated systems.

Comparable abundances between pre-chloraminated (FE) and post-chloraminated (FW-Res) samples suggest that chloramination did not strongly alter nitrifier communities. This might be a consequence of the filters being backwashed with chloraminated water from the FW-Res, promoting the development of similar nitrifier communities in the filter effluent. Continuous ammonia feeding has also been shown to enrich *Nitrosomonas* and *Nitrospira* spp. on filter media (Fujitani et al., 2020). Although backwashing with disinfected water can decrease biofilter diversity and biomass (Bai et al., 2022), the effect of chloraminated backwashing on nitrifiers has received limited study.

Ma et al. (2023) observed that chloraminated backwashing increased AOB abundance and lowered comammox gene concentrations in the effluent compared to filters receiving chlorinated or disinfectant-free backwashes. This finding is consistent with the lower abundance of comammox MAG_589 in the FE observed in this study. It has also been hypothesized that comammox bacteria may prefer a biofilm-bound lifestyle with higher growth rates and greater ammonia affinity (Ma et al., 2023; Koch et al., 2019; Kits et al., 2017). The persistence of comammox MAG_117, closely related to a previously identified Ann Arbor species (Pinto et al., 2016), supports its adaptation to biofilters.

Following chloramination, the abundance of nitrifiers remained stable through the DWDS, suggesting tolerance facilitated by prior exposure in the biofilters through the chloraminated backwash. Pinto et al. (2012) similarly demonstrated that the microbial taxa in the biofilters were present in the FE and throughout the DWDS despite chloramine disinfection. Interestingly, the abundance of comammox MAG_589 increased post-chloramination, particularly in the colder months, suggesting that individual comammox species or strains may occupy distinct ecological niches and exhibit adaptations that influence their persistence and activity in nitrification processes.

4.3. Site-specific factors in the DWDS influence nitrifier abundances

The increased nitrite concentrations at certain DWDS locations during summer and fall may be attributed to several site-specific factors. Literature indicates that the biofilm microbial composition, pipe age and material, and hydraulic conditions, such as low flow or stagnation, can all contribute to localized nitrifier activity and nitrite accumulation (Vikesland et al., 2001; Hossain et al., 2022; Zhang et al., 2009; Cruz et al., 2020; Sung et al., 2005; Bradley et al., 2020). Based on these factors, it is plausible that longer water age and chloramine decay, releasing ammonia, promote nitrite spikes. Such conditions may favor the persistence of nitrifiers, particularly in areas prone to biofilm attachment, corrosion, or solids accumulation, which are generally more common at locations farther from the WTP (Wahman and Pressman, 2014).

The impact of a high water age was evident at Site E, where monochloramine concentrations were low, and ammonia and nitrite concentrations were high, suggesting monochloramine decay. Increased nitrite concentrations in late summer and early fall (September to October) at Site E may be linked to the increase in *Nitrosomonas* abundance, coinciding with a decline in *Nitrospira*-NOB abundance, likely contributing to nitrite accumulation. Comammox MAG_589 also emerged as the most abundant nitrifier at Site E in October. While abundances determined by DNA-based methods do not confirm cell viability or activity, elevated nitrite concentrations indicate ongoing nitrification, potentially influenced by differences in ammonia and nitrite oxidation kinetics, temporal lags, or environmental constraints affecting nitrifier activity (Nowka et al., 2015; Kits et al., 2017; Shao and Wu, 2021; Yan et al., 2024).

The impact of water age was especially apparent for *Nitrosomonas* MAG_097, which exhibited distinct temporal trends compared to other *Nitrosomonas* MAGs and increased as water age increased. In contrast, the drop in *Nitrosomonas* MAG_343 abundance at all three DWDS sites in July underscores the variability in ecological strategies among *Nitrosomonas* spp., reflecting potential differences in ammonia affinity, growth rates, nitrite sensitivity, temperature tolerance, biofilm formation capacity, and competition with comammox for ammonia. These observations highlight the influence of water age and site-specific factors (e.g., biofilm composition and water usage) on nitrifier community structure and nitrification efficiency. Notably, all *Nitrosomonas* MAGs belonged to *Nitrosomonas* cluster 6a, which is typically associated with low-ammonia environments with high substrate affinity and sensitivity to elevated ammonia and nitrite levels (Sedlacek et al., 2019). The distinct spatial and temporal patterns observed here reveal previously unrecognized species- or strain-level ecological adaptations influencing ammonia affinity and nitrification kinetics. Several studies have demonstrated that *Nitrosomonas* cluster 6a spp. thrive under low-ammonia conditions (Bollmann et al., 2013; Potgieter et al., 2020), although direct comparisons of ammonia affinity among these organisms remain limited and warrant further investigation.

4.4. Diversity and ecological niches of drinking water nitrifiers

The two *Nitrospira*-NOB MAGs clustered phylogenetically and exhibited similar abundance patterns, consistent with niche similarity. *Nitrospira* spp. have been observed to co-occur not only with species from the same sublineage but also with clade A comammox *Nitrospira*, highlighting the complex nitrifier dynamics in drinking water systems (Palomo et al., 2022). In this study, such co-occurrence was also evident, particularly at Site E, underscoring their adaptation to drinking water systems and the spatial factors driving niche separation among nitrifiers. Importantly, by resolving species- and clade-level patterns, this study provides higher-resolution ecological insight than is typically available

from 16S rRNA gene-based analyses. While their abundances vary, their dynamics in full-scale drinking water systems warrant further investigation due to diverse treatment strategies and site-specific characteristics of individual DWDS locations. Additionally, microbial communities are often considered part of a continuum in drinking water systems, with the potential for microbial drift through the DWDS. Therefore, the DNA recovered from bulk water at a given location may include organisms (both live and dead) that originated upstream, complicating site-specific interpretations of nitrifier community structure, function, and predicted metabolism. Nonetheless, the observed site-specific variation among nitrifier groups alongside concurrent shifts in nitrite concentrations suggests that these genome-resolved patterns reflect active or persistent populations and reveal ecological differentiation that provides new insight into how nitrifiers coexist and persist under chloraminated conditions.

Seasonal temperature changes likely favor *Nitrospira* (NOB and comammox) and *Nitrosomonas* at different times of the year. Members of *Nitrosomonas* cluster 6a, which are adapted to low-ammonia environments, may dominate at certain times due to their ability to function at low ammonia levels (Bollmann et al., 2013). However, they are sensitive to high nitrite concentrations, particularly in summer and fall. Additionally, *Nitrospira*-comammox have been reported to exhibit higher affinities for ammonia (Koch et al., 2019; Kits et al., 2017), which may explain their comparable or even higher abundances relative to *Nitrosomonas* in the summer and early fall. The coexistence of these nitrifiers may lead to competitive interactions, especially when environmental conditions such as temperature or ammonia concentration fluctuate in the biofilter and DWDS environments. Further, microbial migration in the DWDS can complicate nitrification dynamics, as samples may contain upstream organisms. Similarly, nitrite detected at a site may not be produced locally but could result from upstream nitrification events, complicating site-specific interpretations of microbial nitrification.

5. Conclusion

Effective mitigation of nitrification in chloraminated drinking water systems requires a comprehensive understanding of nitrifier dynamics throughout treatment and distribution. This study's combined use of targeted ddPCR and quantitative genome-resolved metagenomics provided consistent and high-resolution insights into nitrifier population absolute abundances, demonstrating how these tools can inform operational decision-making and support proactive nitrification control. The persistence of nitrifiers from the FE through the DWDS highlights the influence of upstream microbial conditions on downstream community composition. While this study did not directly test operational practices, factors such as biofilm development in biofilters and exposure to chloraminated backwash might allow nitrifiers to withstand disinfection, facilitating their persistence and potential growth in the DWDS. This has direct operational relevance, suggesting that biofilter operation, particularly in full-scale systems that backwash biofilters with chloraminated water, should be considered alongside disinfection practices as part of integrated nitrification control strategies.

Additionally, recognizing the influence of DWDS site-specific factors, such as disinfectant decay, water age, and biofilm development, highlights the need for more targeted interventions to address localized nitrification challenges. Although conducted in a single full-scale utility, the study's biofiltration–chloramination configuration reflects treatment strategies that are increasingly adopted across the industry, particularly in response to evolving regulatory demands. By distinguishing among *Nitrosomonas, Nitrospira*-NOB, and comammox clades, this study reveals species- and clade-level responses to operational and seasonal factors, offering new ecological insight into how nitrifiers coexist and persist under realistic full-scale operational conditions. Therefore, our findings provide broadly transferable insights into nitrifier ecology and control, supporting utilities with similar configurations in designing more effective, data-driven nitrification management strategies. Overall, this work moves beyond showing that treatment influences the distribution system. It provides genome-resolved, quantitative evidence of nitrifier persistence under chloraminated conditions, offering utilities a clearer understanding of how upstream biofiltration practices shape downstream microbial dynamics.

Declaration of generative AI and AI-assisted technologies in the manuscript preparation process

During the preparation of this work, the author(s) used *ChatGPT* (OpenAI) to support language editing and improve clarity of writing. After using this tool/service, the author(s) reviewed and edited the content as needed and take(s) full responsibility for the content of the published article.

CRediT authorship contribution statement

Sarah Potgieter: Writing – original draft, Visualization, Methodology, Investigation, Formal analysis, Data curation, Conceptualization. **Solize Oosthuizen-Vosloo:** Writing – review & editing, Validation, Methodology, Formal analysis, Conceptualization. **Kathryn Langenfeld:** Writing – review & editing, Methodology. **Katherine S. Dowdell:** Writing – review & editing, Methodology, Investigation, Data curation. **Matthew Vedrin:** Writing – review & editing, Methodology, Investigation, Data curation. **Rebecca Lahr:** Writing – review & editing, Conceptualization. **Ameet J. Pinto:** Writing – review & editing, Conceptualization. **Lutgarde Raskin:** Writing – review & editing, Supervision, Resources, Conceptualization.

Declaration of competing interest

The authors declare that they have no known competing financial interests or personal relationships that could have appeared to influence the work reported in this paper.

Given their role as an editor for Water Research, Pinto, A. J. had no involvement in the peer review of this article and had no access to information regarding its peer review. Full responsibility for the editorial process for this article was delegated to another journal editor. If there are other authors, they declare that they have no known competing financial interests or personal relationships that could have appeared to influence the work reported in this paper.

Acknowledgments

The authors gratefully acknowledge the staff and operators of the Ann Arbor WTP and the building owners at the various DWDS sites for their support of this work. Also, special acknowledgement goes to Bridget Hegarty and Zihan Dai for their support with metagenomic data analysis and Soojung Lee for reviewing the manuscript. Funding was provided by the Blue Sky Initiative (College of Engineering, University of Michigan) and the Water Research Foundation (WRF 5151). This research was supported by sequencing performed by the University of Michigan Advanced Genomics Core.

Supplementary materials

Supplementary material associated with this article can be found, in the online version, at doi:10.1016/j.watres.2025.125288.

Data availability

Raw sequence reads are available on NCBI at Bioproject number PRJNA1081894.

References

Andersson, A., Laurent, P., Kihn, A., Prévost, M., Servais, P., 2001. Impact of temperature on nitrification in biological activated carbon (BAC) filters used for drinking water treatment. Water. Res. 35 (12), 2923–2934.

Bai, X., Dinkla, I.J., Muyzer, G., 2022. Microbial ecology of biofiltration used for producing safe drinking water. Appl. Microbiol. Biotechnol. 106 (13), 4813–4829.

Basu, O.D., Dhawan, S., Black, K., 2016. Applications of biofiltration in drinking water treatment–a review. J. Chem. Technol. Biotechnol. 91 (3), 585–595.

Bollmann, A., Sedlacek, C.J., Norton, J., Laanbroek, H.J., Suwa, Y., Stein, L.Y., Klotz, M. G., Arp, D., Sayavedra-Soto, L., Lu, M., Bruce, D., 2013. Complete genome sequence of *nitrosomonas* sp. Is79, an ammonia oxidizing bacterium adapted to low ammonium concentrations. Stand. Genom. Sci. 7, 469–482.

Bond, T., Huang, J., Templeton, M.R., Graham, N., 2011. Occurrence and control of nitrogenous disinfection by-products in drinking water–a review. Water. Res. 45 (15), 4341–4354.

Bougeard, C.M.M., Goslan, E.H., Jefferson, B., Parsons, S.A., 2010. Comparison of the disinfection by-product formation potential of treated waters exposed to chlorine and monochloramine. Water. Res. 44 (3), 729–740.

Bowers, R.M., Kyrpides, N.C., Stepanauskas, R., Harmon-Smith, M., Doud, D., Reddy, T. B.K., Schulz, F., Jarett, J., Rivers, A.R., Eloe-Fadrosh, E.A., Tringe, S.G., 2017. Minimum information about a single amplified genome (MISAG) and a metagenome-assembled genome (MIMAG) of bacteria and archaea. Nat. Biotechnol. 35 (8), 725–731.

Bradley, T.C., Haas, C.N., Sales, C.M., 2020. Nitrification in premise plumbing: a review. Water 12 (3), 830.

Cruz, M.C., Woo, Y., Flemming, H.C., Wuertz, S., 2020. Nitrifying niche differentiation in biofilms from full-scale chloraminated drinking water distribution system. Water. Res. 176, 115738.

Daims, H., Lebedeva, E.V., Pjevac, P., Han, P., Herbold, C., Albertsen, M., Jehmlich, N., Palatinszky, M., Vierheilig, J., Bulaev, A., Kirkegaard, R.H., 2015. Complete nitrification by *Nitrospira* bacteria. Nature 528 (7583), 504–509.

Daims, H., Lücker, S., Wagner, M., 2016. A new perspective on microbes formerly known as nitrite-oxidizing bacteria. Trends. Microbiol. 24 (9), 699–712.

Dionisi, H.M., Layton, A.C., Harms, G., Gregory, I.R., Robinson, K.G., Sayler, G.S., 2002. Quantification of *Nitrosomonas oligotropha*-like ammonia-oxidizing bacteria and *nitrospira* spp. From full-scale wastewater treatment plants by competitive PCR. Appl. Environ. Microbiol. 68 (1), 245–253.

Dowdell, K.S., Potgieter, S.C., Olsen, K., Lee, S., Vedrin, M., Caverly, L.J., LiPuma, J.J., Raskin, L., 2024. Source-to-tap investigation of the occurrence of nontuberculous mycobacteria in a full-scale chloraminated drinking water system. Appl. Environ. Microbiol. 90 (9), e00609–e00624.

European Union (EU), 2020. Directive (EU) 2020/2184 of the European Parliament and of the Council of December 16. on the quality of water intended for human consumption Off. J. Eur. Union 435, 1–62.

Fowler, S.J., Palomo, A., Dechesne, A., Mines, P.D., Smets, B.F., 2018. Comammox *Nitrospira* are abundant ammonia oxidizers in diverse groundwater-fed rapid sand filter communities. Environ. Microbiol. 20 (3), 1002–1015.

Fujitani, H., Momiuchi, K., Ishii, K., Nomachi, M., Kikuchi, S., Ushiki, N., Sekiguchi, Y., Tsuneda, S., 2020. Genomic and physiological characteristics of a novel nitrite-oxidizing Nitrospira strain isolated from a drinking water treatment plant. Front. Microbiol. 11, 545190.

nov. In Garrity, G.M., Bell, J.A., Lilburn, T., Order, V., Nitrosomonadales, 2005. In: Brenner, D.J., Krieg, N.R., Staley, J.T. (Eds.), Editors. Bergey's Manual of Systematic Bacteriology, Editors. Bergey's Manual of Systematic Bacteriology, 2nd ed., 2. Springer-Verlag, Heidelberg, pp. 863–886. The Proteobacteria (Part C); The Alpha-, Beta-, Delta-, and Epsilonproteobacteria.

Goel, S., Hozalski, R.M., Bouwer, E.J., 1995. Biodegradation of NOM: effect of NOM source and ozone dose. J. Am. Water Work. Assoc. 87 (1), 90–105.

Hardwick, S.A., Chen, W.Y., Wong, T., Kanakamedala, B.S., Deveson, I.W., Ongley, S.E., Santini, N.S., Marcellin, E., Smith, M.A., Nielsen, L.K., Lovelock, C.E., 2018. Synthetic microbe communities provide internal reference standards for metagenome sequencing and analysis. Nat. Commun. 9 (1), 3096.

Harms, G., Layton, A.C., Dionisi, H.M., Gregory, I.R., Garrett, V.M., Hawkins, S.A., Robinson, K.G., Sayler, G.S., 2003. Real-time PCR quantification of nitrifying bacteria in a municipal wastewater treatment plant. Environ. Sci. Technol. 37 (2), 343–351.

Hermansson, A., Lindgren, P.E., 2001. Quantification of ammonia-oxidizing bacteria in arable soil by real-time PCR. Appl. Environ. Microbiol. 67 (2), 972–976.

Hossain, S., Chow, C.W., Cook, D., Sawade, E., Hewa, G.A., 2022. Review of chloramine decay models in drinking water system. Environ. Sci.: Water Res. Technol. 8 (5), 926–948.

Huggett, J.F., 2020. The digital MIQE guidelines update: minimum information for publication of quantitative digital PCR experiments for 2020. Clin. Chem. 66 (8), 1012–1029.

Itoh, Y., Sakagami, K., Uchino, Y., Boonmak, C., Oriyama, T., Tojo, F., Matsumoto, M., Morikawa, M., 2013. Isolation and characterization of a thermotolerant ammonia-oxidizing bacterium *Nitrosomonas* sp. JPCCT2 from a thermal power station. Microbes. Environ. 28 (4), 432–435.

Kits, K.D., Sedlacek, C.J., Lebedeva, E.V., Han, P., Bulaev, A., Pjevac, P., Daebeler, A., Romano, S., Albertsen, M., Stein, L.Y., Daims, H., 2017. Kinetic analysis of a complete nitrifier reveals an oligotrophic lifestyle. Nature 549 (7671), 269–272.

Koch, H., van Kessel, M.A., Lücker, S., 2019. Complete nitrification: insights into the ecophysiology of comammox Nitrospira. Appl. Microbiol. Biotechnol. 103, 177–189.

Kotlarz, N., Rockey, N., Olsen, T.M., Haig, S.J., Sanford, L., LiPuma, J.J., Raskin, L., 2018. Biofilms in full-scale drinking water ozone contactors contribute viable bacteria to ozonated water. Environ. Sci. Technol. 52 (5), 2618–2628.

Kozlowski, J.A., Kits, K.D., Stein, L.Y., 2016. Complete genome sequence of *nitrosomonas ureae* strain Nm10, an oligotrophic group 6a nitrosomonad. Genome Announc. 4 (2), 10–1128.

Langenfeld, K., Hegarty, B., Vidaurri, S., Crossette, E., Duhaime, M.B., Wigginton, K.R., 2025. Development of a quantitative metagenomic approach to establish quantitative limits and its application to viruses. Nucleic. Acids. Res. 53 (5), gkaf118.

LaPara, T.M., Hope Wilkinson, K., Strait, J.M., Hozalski, R.M., Sadowksy, M.J., Hamilton, M.J., 2015. The bacterial communities of full-scale biologically active, granular activated carbon filters are stable and diverse and potentially contain novel ammonia-oxidizing microorganisms. Appl. Environ. Microbiol. 81 (19), 6864–6872.

Laurent, P., Kihn, A., Andersson, A., Servais, P., 2003. Impact of backwashing on nitrification in the biological activated carbon filters used in drinking water treatment. Environ. Technol. 24 (3), 277–287.

Lee, W.H., Wahman, D.G., Bishop, P.L., Pressman, J.G., 2011. Free chlorine and monochloramine application to nitrifying biofilm: comparison of biofilm penetration, activity, and viability. Environ. Sci. Technol. 45 (4), 1412–1419.

Ma, B., LaPara, T.M., Hozalski, R.M., 2020. Microbiome of drinking water biofilters is influenced by environmental factors and engineering decisions but has little influence on the microbiome of the filtrate. Environ. Sci. Technol. 54 (18), 11526–11535.

Ma, B., LaPara, T.M., Kim, T., Hozalski, R.M., 2023. Multi-scale investigation of ammonia-oxidizing microorganisms in biofilters used for drinking water treatment. Environ. Sci. Technol. 57 (9), 3833–3842.

National Research Council, 1995. Nitrate and Nitrite in Drinking Water. National Academy Press.

Nowka, B., Daims, H., Spieck, E., 2015. Comparison of oxidation kinetics of nitrite-oxidizing bacteria: nitrite availability as a key factor in niche differentiation. Appl. Environ. Microbiol. 81 (2), 745–753.

Oksanen, J., Blanchet, F.G., Friendly, M., Kindt, R., Legendre, P., McGlinn, D., Minchin, P.R., O'hara, R.B., Simpson, G.L., Solymos, P., Stevens, M.H.H., 2019. Vegan: community ecology package. R Packag. Version 2 (10).

Orschler, L., Agrawal, S., Lackner, S., 2020. Lost in translation: the quest for *Nitrosomonas* cluster 7-specific *amoA* primers and TaqMan probes. Microb. Biotechnol. 13 (6), 2069–2076.

Palomo, A., Dechesne, A., Pedersen, A.G., Smets, B.F., 2022. Genomic profiling of *Nitrospira* species reveals ecological success of comammox *Nitrospira*. Microbiome 10 (1), 204.

Pintar, K.D., Slawson, R.M., 2003. Effect of temperature and disinfection strategies on ammonia-oxidizing bacteria in a bench-scale drinking water distribution system. Water. Res. 37 (8), 1805–1817.

Pinto, A.J., Xi, C., Raskin, L., 2012. Bacterial community structure in the drinking water microbiome is governed by filtration processes. Environ. Sci. Technol. 46 (16), 8851–8859.

Pinto, A.J., Marcus, D.N., Ijaz, U.Z., Bautista-de los Santos, Q.M., Dick, G.J., Raskin, L., 2016. Metagenomic evidence for the presence of comammox *nitrospira*-like bacteria in a drinking water system. mSphere 1 (1) e00054-15.

Potgieter, S.C., Dai, Z., Venter, S.N., Sigudu, M., Pinto, A.J., 2020. Microbial nitrogen metabolism in chloraminated drinking water reservoirs. mSphere 5 (2), 10–1128.

Potgieter, S., Lee, S., Raskin, L., Lahr, B., Steglitz, B., 2025. Impact of UV Treatment on Microbial Communities in a Full-Scale Drinking Water Distribution System. Project 5151. Water Research Foundation, Denver, CO.

R Core Team, 2021. R: a language and environment for statistica computing. R Foundation for Statistical Computing. URL. https://www.R-project.org/.

Rosenqvist, T., Danielsson, M., Schleich, C., Ahlinder, J., Brindefalk, B., Pullerits, K., Dacklin, I., Salomonsson, E.N., Sundell, D., Forsman, M., Keucken, A., 2023. Succession of bacterial biofilm communities following removal of chloramine from a full-scale drinking water distribution system. NPJ. Clean. Water. 6 (1), 41.

Rossman, L., Woo, H., Tryby, M., Shang, F., Janke, R., Haxton, T., 2020. EPANET (2.2.0). U.S. Environmental Protection Agency, Washington, DC, USA.

RStudio Team, 2020. RStudio: Integrated Development for R. RStudio.

Sakoula, D., Nowka, B., Spieck, E., Daims, H., Lücker, S., 2018. The draft genome sequence of "nitrospira lenta" strain BS10, a nitrite-oxidizing bacterium isolated from activated sludge. Stand. Genom. Sci. (13), 32.

Sakoula, D., Koch, H., Frank, J., Jetten, M.S., van Kessel, M.A., Lücker, S., 2021. Enrichment and physiological characterization of a novel comammox *Nitrospira* indicates ammonium inhibition of complete nitrification. ISMe J. 15 (4), 1010–1024.

Sedlacek, C.J., McGowan, B., Suwa, Y., Sayavedra-Soto, L., Laanbroek, H.J., Stein, L.Y., Norton, J.M., Klotz, M.G., Bollmann, A., 2019. A physiological and genomic comparison of *Nitrosomonas* cluster 6a and 7 ammonia-oxidizing bacteria. Microb. Ecol. 78, 985–994.

Shao, Y.H., Wu, J.H., 2021. Comammox *Nitrospira* species dominate in an efficient partial nitrification–anammox bioreactor for treating ammonium at low loadings. Environ. Sci. Technol. 55 (3), 2087–2098.

Shi, Y., Babatunde, A., Bockelmann-Evans, B., Li, Q., Zhang, L., 2020. On-going nitrification in chloraminated drinking water distribution system (DWDS) is conditioned by hydraulics and disinfection strategies. J. Environ. Sci. 96, 151–162.

Sung, W., Huang, X., Wei, I.W., 2005. Treatment and distribution system effects on chloramine decay, pH, nitrification, and disinfection by-products: case study. J. Water. Resour. Plan. Manag. 131 (3), 201–207.

Tatari, K., Musovic, S., Gülay, A., Dechesne, A., Albrechtsen, H.J., Smets, B.F., 2017. Density and distribution of nitrifying guilds in rapid sand filters for drinking water production: dominance of *Nitrospira* spp. Water. Res. 127, 239–248.

US EPA. National Primary Drinking Water Regulations. Accessed 12/05/2024. https://www.epa.gov/ground-water-and-drinking-water/national-primary-drinking-water-regulations.
Vikesland, P.J., Ozekin, K., Valentine, R.L., 2001. Monochloramine decay in model and distribution system waters. Water. Res. 35 (7), 1766–1776.
Vilardi, K.J., Cotto, I., Sevillano, M., Dai, Z., Anderson, C.L., Pinto, A., 2022. Comammox Nitrospira bacteria outnumber canonical nitrifiers irrespective of electron donor mode and availability in biofiltration systems. FEMS. Microbiol. Ecol. 98 (4), fiac032.
Vosloo, S., Sevillano-Rivera, M., Pinto, A.J., 2019. Modified DNeasy PowerWater Kit® Protocol for DNA Extractions from Drinking Water Samples. Protocolsio.
Vosloo, S., Huo, L., Anderson, C.L., Dai, Z., Sevillano, M., Pinto, A., 2021. Evaluating de Novo Assembly and binning strategies for time series drinking water metagenomes. Microbiol. Spectr. 9 (3) e01434-21.
Wahman, D.G., Pressman, J.G., 2014. Nitrification in chloraminated drinking water distribution systems: factors affecting occurrence. *Compr. Water Qual. Purif.* 2, 283–294.
Wang, Y., Ma, L., Mao, Y., Jiang, X., Xia, Y., Yu, K., Li, B., Zhang, T., 2017. Comammox in drinking water systems. Water. Res. 116, 332–341.
Wickham, H., Chang, W., Wickham, M.H., 2016. Package 'ggplot2'. Create elegant data visualisations using the grammar of graphics. R Packag. Version 2 (1), 1–189.
Wilczak, A., Jacangelo, J.G., Marcinko, J.P., Odell, L.H., Kirmeyer, G.J., 1996. Occurrence of nitrification in chloraminated distribution systems. J.-Am. Water Work. Assoc. 88 (7), 74–85.
World Health Organization, 2017. Guidelines for Drinking-Water quality: Fourth Edition Incorporating the First Addendum. World Health Organization, Geneva. https://www.who.int/publications/i/item/9789241549950.
Yan, Y., Lee, J., Han, I.L., Wang, Z., Li, G., McCullough, K., Klaus, S., Kang, D., Wang, D., Patel, A., McQuarrie, J., 2024. Comammox and unknown ammonia oxidizers contribute to nitrite accumulation in an integrated AB stage process that incorporates side-stream EBPR (S2EBPR). Water. Res. 253, 121220.
Yang, X., Yu, X., He, Q., Deng, T., Guan, X., Lian, Y., Xu, K., Shu, L., Wang, C., Yan, Q., Yang, Y., 2022. Niche differentiation among comammox (*Nitrospira inopinata*) and other metabolically distinct nitrifiers. Front. Microbiol. 13, 956860.
Yuichi, S., Norton, J.M., Bollmann, A., Klotz, M.G., Stein, L.Y., Laanbroek, H.J., Arp, D.J., Goodwin, L.A., Chertkov, O., Held, B., Bruce, D., 2011. Genome sequence of *nitrosomonas* sp. strain AL212, an ammonia-oxidizing bacterium sensitive to high levels of ammonia. J. Bacteriol. 193, 5047–5048.
Zhang, Y., Love, N., Edwards, M., 2009. Nitrification in drinking water systems. Crit. Rev. Environ. Sci. Technol. 39 (3), 153–208.